



Alexandria University  
**Alexandria Engineering Journal**

[www.elsevier.com/locate/aej](http://www.elsevier.com/locate/aej)  
[www.sciencedirect.com](http://www.sciencedirect.com)



# Dynamic simulation and exergetic analysis of a solar thermal collector installation



David García-Menéndez<sup>a</sup>, Juan Carlos Ríos-Fernández<sup>a,\*</sup>,  
 Ana María Blanco-Marigorta<sup>b</sup>, María José Suárez-López<sup>a</sup>

<sup>a</sup> Universidad de Oviedo, EDZE (Energía), Campus de Viesques, 33203 Gijón (Asturias), Spain

<sup>b</sup> Universidad de Las Palmas de Gran Canaria, Department of Process Engineering, Tafira Baja s/n, Las Palmas de G.C., Canary Islands, Spain

Received 2 March 2021; revised 7 May 2021; accepted 20 June 2021  
 Available online 01 July 2021

## KEYWORDS

Solar thermal collector;  
 Exergetic analysis;  
 TRNSYS dynamic model;  
 Exergetic efficiency

**Abstract** Solar collectors are active solar devices which help reducing the energy consumption in buildings. In this paper, a real installation of solar collectors is analysed under different collector array configurations. Also, both energetic and exergetic analyses have been developed, for both general balance and specific variables. To apply these analyses, a TRNSYS dynamic model has been built and validated with experimental data obtained in the real installation. The values of the representative variables have been examined in different points of the installation, resulting in a description of the installation operation and parameters influencing the exergetic efficiency. Although parallel connections of the collectors are commonly used, in this work, simulations and experiments have been carried out with both parallel and series connections. As a result, no significant differences regarding the array configurations have been found. The values of the exergetic efficiency of the collectors are always very low (within 1% and 4.6%), no matter the configuration nor the irradiance. Its maximum value was reached after about 5 h of operation, for all configurations. The values obtained for the whole installation are in the range of 20–50% for the energetic efficiency, whereas the exergetic efficiency is always lower than 1.5%.

© 2021 THE AUTHORS. Published by Elsevier BV on behalf of Faculty of Engineering, Alexandria University. This is an open access article under the CC BY license (<http://creativecommons.org/licenses/by/4.0/>).

## 1. Introduction

In the current energy situation, with a growing use of renewable energy and the consequent reduction of gas emissions, thermal solar energy is one of the most popular alternatives

in households, both for a single dwelling [1,2] and for a larger scale (such as district heating systems) [3,4]. Among the diverse alternatives, solar collectors are widely used and, specifically, flat-plate solar collectors are the most common ones throughout the world [5] due to their characteristics (simple design, compactness, low production and maintenance cost) and their reliability obtained through long years of experience, research and development [6,7].

Several studies carried out on flat-plate collectors have been focused on thermal performance using laboratory or prototype

\* Corresponding author.

E-mail address: [riosjuan@uniovi.es](mailto:riosjuan@uniovi.es) (J.C. Ríos-Fernández).

Peer review under responsibility of Faculty of Engineering, Alexandria University.

**Nomenclature**

$A$	Surface, m <sup>2</sup>	$i$	$i$ -th material stream
$c$	Heat capacity, kJ/K·kg	$j$	$j$ -th instant
$ex$	Specific exergy, kJ/kg	$in$	inlet
$\dot{E}_x$	Exergy flow rate, kW	$k$	$k$ -th component
$h$	Specific enthalpy, kJ/kg	$KN$	Kinetic
$I$	Solar irradiance, W/m <sup>2</sup>	$L$	Loss
$in$	Inlet	$out$	outlet
$\dot{m}$	Mass flow rate, kg/s	$P$	Product
$\eta$	Efficiency	$p$	Pressure
$out$	Outlet	$PH$	Physical
$p$	Pressure, kPa	$PT$	Potential
$\dot{Q}$	Heat transfer flow rate, kW	$Q$	Heat transfer
$R$	Universal gas constant, kJ/ K·kmol	$s$	Sun
$s$	Specific entropy, kJ/K·kg	$sr$	Solar radiation
$T$	Temperature, K	$tot$	Total
Subscripts and superscripts $0$		Abbreviations	
	Dead state	$EES$	Engineering equation Solver
$c$	Collector	$GSCL$	Gijón Solar Cooling Laboratory
$CH$	Chemical	$HX$	Heat exchanger
$D$	Destruction	$TIM$	Transparent Insulation Materials
$ex$	Exergetic	$TRNSYS$	Transient Systems Simulation Program
$F$	Fuel		

installations [6,8,9], making experimental tests with a single collector. Verna et al. [6] evaluated the improvement of the performance substituting the water as thermal fluid by nanofluids. Álvarez et al. [9] presented a new design characterized by its corrugated channel and by the high surface area directly in contact with the heat transport fluid. This design was evaluated using both an experimental analysis and a thermal and hydrodynamic model. Zambolin and Del Col [8] compared the efficiency of a standard glazed flat plate collector and an evacuated tube collector according to the European normative. In these small installations, it is not feasible to create all testing environments due to excessive run duration, trade off and socio-financial implications, as Shivastava et al. [10] and Tagliafico et al. [11] pointed out. In such cases, both modelling and simulation are good alternatives for performing long-term analyses under different weather and operating conditions, and design optimizations. Shivastava et al. [10] carried out a review on different simulation tools for these systems and considered that TRNSYS can be a good option because this tool enables to simulate the whole solar installation, including the main elements (solar collectors and water storage tanks) and the secondary elements (pumps, pipes, and so on).

Also, TRNSYS is one of the tools subjected to continuous revisions and updates. Regarding the dynamic simulations, there are several papers analysing larger scale installations and different climates. Ayompe et al. [2] developed a simulation model for forced circulation solar water heating systems. This model was validated with experimental data taken in an installation composed of two flat-plate collectors and a heat pipe evacuated tube collector and produced hot water for a typical European domestic dwelling in a temperate climate. The model underestimated the collector outlet fluid temperature by  $-9.6\%$ . Hobbi and Siddiqui [11] performed a TRNSYS model for an

indirect forced circulation solar water system using a flat-plate collector, producing hot water requirements of a single-family residential unit in a cold climate. Sokhansefat et al. [12] compared two different solar hot water systems with two types of solar collectors (flat-plate and evacuated tube) under cold climate conditions, using a TRNSYS model validated with experimental data. They obtained the absolute value error of the outlet temperature and the mean energy efficiency in a year. For this type of climate, the evacuated tube collectors have higher performance. Also, there are some studies of large solar thermal plants for district heating, although they are still scarce. Bava and Furbo [3] presented a detailed TRNSYS-Matlab model to simulate a large solar collector field for district heating application, comparing the results with experimental data. They studied different parameters such as the flow distribution in the different rows, the effect of the flow regime on the collector efficiency, and so on. Tiwari et al. [13] used TRNSYS to simulate flat plate collectors in India observing a worse performance of the installation in the monsoon season, July and August. Recently, Harrabi et al. [14] analysed the performance of a thermosyphon flat-plate solar installation to produce domestic hot water in a residential dwelling in Tunisia, using a dynamic model developed in TRNSYS. The results of the simulations pointed out that with higher storage volume, higher efficiency and solar fractions were achieved. Tian et al. [15] analysed and validated a solar collector field with both flat plate and parabolic trough collectors for district heating. In all the references found in the literature it is assumed parallel connection between solar collectors, omitting the possibility of serial connection.

The concept of energy quality is naturally associated with exergy. In this way, exergy analysis can be used in parallel with energy analysis to determine the most efficient use of energy. Several authors have applied the methodology of exergetic

analysis for the optimization of a single flat-plate solar collector. Gunerhan and Hepbasli [16] investigated a solar water heating system consisting of a flat plate collector and analysed the influence of the water inlet temperature on the exergetic efficiency of the collector. Farahat et al. [17] performed an exergetic optimization of flat plate solar collectors to determine design parameters and the optimal thermal and optical performance of the collectors. They found the maximum exergetic efficiency, as well as the optimum values of the absorber plate area and the mass flow rate. Pons [18] carried out a comprehensive exergetic study of the solar collectors, taking into account both direct and diffuse solar radiation, and calculating the exergy losses in the flat-type solar collectors. Jafarkazemi and Ahmadifard [19] presented both energetic and exergetic evaluations of this solar technology analysing the effect of the design parameters (working fluid, mass flow rate, inlet temperature, and thickness of the back insulation) on the performance. The same design parameters were analysed in the work of Chamoli [20] with the application of an optimization procedure of a typical flat-plate solar collector based on exergy analysis. Ge et al. [21] introduced, and experimentally validated, a theoretical exergetic model for the analysis of flat plate solar collectors, which considers the lack of uniformity in the temperature distribution along the absorber plate. Mortazavi and Ameri [22] performed both a conventional and an advanced exergetic analysis on a simple flat plate collector and a flat plate collector with thin metal sheet. They investigated the effect of the radiation, the channel depth and the Reynolds number on the exergy destruction of each flat-plate configuration components. Genc et al. [23] presented a transient numerical heat transfer approach for determining the thermal inertia of each component of a nanofluid flat plate solar collector. Through an exergy analysis, they evaluated the effect of operation parameters on the thermal efficiency of the collector.

However, few studies addressed the exergetic evaluation of flat-plate solar collector arrays together with processes related to the conditioning of buildings. Kalogirou et al. [24] provided a review on exergy analysis of solar thermal collectors and processes, including flat plate collectors and several water heating applications, where this gap becomes apparent. At the same time, they emphasized that exergy analysis is a valuable method to evaluate and compare possible configurations of these systems and processes. Rosiek [25] reported an exergy analysis carried out on a process combining a flat-plate-collector array together with a single effect LiBr-H<sub>2</sub>O refrigeration system. This work used experimental data from a facility in operation and it concluded with some recommendations, from the exergetic point of view, for the operation parameters. A recent review of Sakhaei and Valipour [26] collects the research conducted on the thermal performance enhancement of flat-plate solar collectors. They introduce some thermal models, based on exergy analysis, for the determination of the optimal design of the collector, and they suggest the use of dynamic models and the comparison of their results with experimental data to choose the best option in modelling of flat-plate solar collectors. In this regard, Allouhi et al. [27] used exergy analysis to analyse the efficiency of a promising alternative where they integrated heat pipes to flat plate collectors as a mean of heat extraction devices. Also, the thermal behaviour of the whole system and its daily energetic and exergetic performances were discussed. Their results showed thermal efficiencies of up to 33% and exergetic efficiencies of up to 4%.

In this paper, a real installation of flat-plate solar collectors located in Gijón (a coastal city in the north of Spain) is analysed. It is part of the Gijón Solar Cooling Laboratory (GSCL) at the University of Oviedo. This laboratory has been designed to test different devices, such as solar collectors, absorption coolers, boilers, ground-coupled heat exchangers and other dissipation systems, used in heating and cooling systems for residential buildings. In order to obtain a highly efficient system, it is very important to evaluate different configurations of the solar collectors and select the most appropriate one. Nonetheless, most home heating installations are designed by using the worst-case approach, the worst environmental conditions in this context. This achieves that the installation works correctly in the worst possible scenario, but it also generates an over-cost of energy and a high level of emissions, unnecessary in most cases. In the present research, a dynamic model for the flat-plate solar collectors is developed using TRNSYS. Both the primary and the secondary circuits are modelled, and the experimental tests carried out in the real installation are used to validate the model. After the validation, six configurations of the flat-plate solar collectors are simulated, under five different normal irradiance conditions (200, 400, 600, 800 and 1000 W/m<sup>2</sup>), giving a total of 30 cases. The main parameters are obtained to analyse the performance. Furthermore, both energetic and exergetic analyses have been performed, for both general balance and specific variables.

The novelty and main contributions of this paper are:

1. Developing a detailed TRNSYS model of a real installation of 20 flat-plate solar collectors (considering both the main and secondary devices) and its validation with experimental data (as we have already considered, most of the works present in literature are focused on the analysis of a flat-plate solar collector as a single unit, and mainly taking into account theoretical data).
2. Analysing six different possible configurations, through this model with combination of series or parallel connections of the collectors. The performance of the installation has been obtained varying the solar radiation conditions,
3. Choosing the most suitable configuration through energy and exergy analysis. Energetic and exergetic efficiencies have been obtained for all configurations under the different irradiance conditions. This way, the most appropriate scenario has been selected.

This paper is structured as follows: [Section 1](#) contains the introduction and the state of the art on solar thermal collectors. In [Section 2](#) the experimental installation used in this research is described. In [Section 3](#) the dynamic model developed is analysed and validated with experimental data; also, the simulations are performed. In [Section 4](#) the exergetic study is presented. [Section 5](#) discusses the results obtained in the energetic and exergetic analyses by using the dynamic simulations. And finally, in [Section 6](#), the conclusions of this research are presented.

## 2. Experimental installation

A real installation of solar thermal collectors has been used for the experimental tests. This installation is composed of 20 collectors, with a total area of 38.2 m<sup>2</sup>, and which can supply

30 kW of thermal power. This installation is part of the Gijón Solar Cooling Laboratory (GSCL) at the University of Oviedo. It is located in the upper part of the East Department Building at the University Campus of Gijón, a coastal city in the North of Spain, with a yearly insolation of 1700 sunshine hours. Fig. 1 shows a real photograph of the solar thermal field.

The solar thermal collectors have been installed with a slope of  $43^\circ$  towards the South-Southeast, at the coordinates  $43^\circ 31' 21.08''$  Latitude N and  $5^\circ 37' 19.57''$  Longitude W. The solar thermal collectors are flat-plate type, Unisol 90 Clima TIM, dimensions  $2.02 \times 1.02$  m. They have a TIM convective barrier consisting of a cellulose acetate with a honeycomb structure attached to the glass. This technology destroys the cells formed in the collector by convection reducing the thermal losses and increasing their efficiency.



Fig. 1 Photograph of the solar thermal collectors located in the upper part of the East Department Building at the University of Oviedo.

Three-way valves have been installed so that the collectors can be connected in parallel or in series. Thus, different configurations can be studied in order to select the most appropriate one, according to the climatic conditions. Also, there is an inverted return pipe equalizing the paths and, consequently, the head losses, encouraging the hydraulic balancing of the installation.

The installation has two circuits, which have been represented in Fig. 2. The primary or hydraulic circuit is composed of a pumping group (Grundfos TPE 32-180/2 AFA RUUE 1X230), a flowmeter (KOBOLD DMH-1A15T10A10) and the security elements needed. The fluid circulating inside this circuit is a mixture of water and ethylene glycol in a 30% proportion, with a freezing temperature of  $-17^\circ\text{C}$ . This circuit is connected to the secondary one by means of a plate heat exchanger, model UFO-34/19H-C-PN16 (SEDICAL) with 30 kW thermal power. The secondary circuit is composed of a pumping group (Grundfos TPE 32-180/2 AFA RUUE 1X230), a flowmeter (KOBOLD DMH-1A15T10A10) and two water tanks in series with a total volume of 3000 L.

There is also an emergency and safety emptying system, which allows the installation to be emptied in case of long periods of inactivity. It is composed of safety valves, deaerators and an expansion vessel of 300 L.

As regards instrumentation and control, the installation has a pyranometer, and both temperature and pressure sensors in different points, as Fig. 2 shows. For better control of the installation operation, the temperature is measured at the inlet and exit of each collector. All these measurements have been monitored and collected using an acquisition data system of National Instruments.

Different configurations of the solar thermal collectors were tested: 10 groups in parallel of 2 collectors connected in series, 5 groups in parallel of 4 collectors connected in series and 4 groups in parallel of 5 collectors connected in series. For all configurations, different flow rates were used during the experiments, and the temperature at the inlet and exit of each collector, the ambient temperature, the solar radiation and the

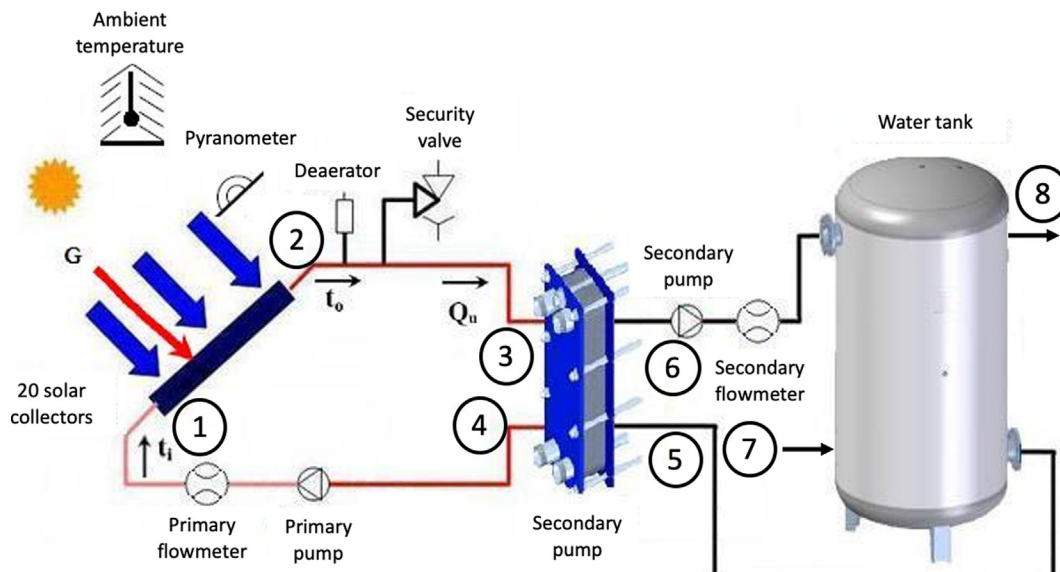


Fig. 2 Scheme of the experimental installation.

volumetric flow rate were measured and registered each 10 s. All the experiments lasted around 1 h. After analysing the experimental results, the configuration of 5 groups in parallel of 4 collectors connected in series was used to validate the model.

### 3. Dynamic model

#### 3.1. Description of the model

The solar thermal installation has been modelled with TRNSYS 17.02.0004, which has been widely used for this purpose [10]. In Fig. 3 it is shown the scheme of the model used for validation with the experiments, where 20 solar collectors were disposed in 4 parallel branches of 5 collectors in series.

The solar collectors were originally checked by the manufacturer according to EN 12975-2:2006 standard, obtaining an intercept efficiency of 0.773, an efficiency slope of 3.071, and an efficiency curvature of 0.015. The collectors were modelled by means of Type 1b [28] (mathematical reference), assuming the intercept efficiency of the tests, but modifying the values of the slope and the curvature of the efficiency, taking into account the effects of the higher convection losses due to wind of 1.3 m/s in the real installation. Thus, values of efficiency slope of 7.75 and efficiency curvature of 0.035 were assumed.

The water storage tanks were modelled with Type 38 [28], considered as a unique tank of 3000 L. Regarding the heat exchanger, it was assumed with constant effectiveness as in Type 91 [28]. As effectiveness, the mean value obtained in the experiments, 0.821 was used. The model also considers pipes with their thermal insulation by means of Type 31 [28].

As input of the model, the solar irradiance on the collector surface, the mass flow rate, and the solar collector inlet temperature are considered by means of Type 9C, generic data reader (Input data in Fig. 3a). The evolution of such variables during the test can be seen in Fig. 4.

Instantaneous ambient temperatures were not registered, but on the day of the experiments a minimum ambient temperature of 16.3 °C and a maximum ambient temperature of 21.6 °C were observed. The test were carried out between 11:15 and 12:17, a value of 19 °C was assumed.

Finally, the time step of the model was set at 10 s, as in the experimental measurements.

#### 3.2. Validation of the model

For the validation of the model, the output temperature of the solar collector array and the thermal power supplied by the collectors are compared with the experimental results (Fig. 5 and Fig. 6). The coupling observed by the model and experimental curves is widely acceptable.

Integrating the thermal power along the experimental time period, the total energy gained in both cases, simulation and experimental tests, is obtained. The total energy produced with the solar array, is 1678.2 kJ for the simulation and 1652.5 kJ for the experiments, resulting in an error of 1.56% for the one-hour test. This result shows reasonable accuracy compared with the values of 14% obtained by Ayompe et al. [1] with TRNSYS simulations for flat-plate collectors in a similar installation. In a district heating facility, Bava and Furgo [3]

obtained discrepancies between simulations and experimental results in the range of 1.7–3.5% for cloudy days and lower than 1% with clear sky conditions. Tian et al. [15] also modeled flat-plate solar collectors with daily energy output fitting experimental results in the range of –1.7% and 1.1%. The same authors reported discrepancies in the range of 3% to 3.9% when simulating the performance of a parabolic trough collectors' field.

#### 3.3. Description of the dynamic simulations

Once the model has been validated, six possible configurations of the solar collector array (Fig. 7) have been modelled and simulated under five different normal irradiance conditions (200, 400, 600, 800 and 1000 W/m<sup>2</sup>), giving a total of 30 cases. Cases are named using a number to identify the array configuration and a letter referring to the irradiation level according to Table 1. Thus, Case 4D corresponds to a collector array of 4 branches of 5 collectors in series under normal irradiance of 800 W/m<sup>2</sup>.

In all the cases, both primary and secondary mass flow rates have been kept constant at 800 kg/h, and the supply water mass flow rate has been considered constant at a value of 90 kg/h. For the calculation of the supply water flow rate, the typical requirement for twelve families, where 75 L per family and per day are demanded, has been assumed. The replacing water coming into the tank has been considered at 19 °C (ambient temperature). The simulations have been run over a period of 10 h, with a simulation time step of 1 min.

### 4. Exergetic analysis

An exergy balance can be applied to this installation following the general formulation [29]:

$$\sum \dot{E}x_{in} = \sum \dot{E}x_{out} + \dot{E}x_D + \dot{E}x_L \quad (1)$$

In this balance, the inlet and outlet terms account for the exergy associated with both material and energy transfers.

In this solar collector installation, just material and heat transfers can occur. The exergy rate associated with a heat transfer is [29]:

$$\dot{E}x_{Q,j} = \left(1 - \frac{T_0}{T_j}\right) \dot{Q}_j \quad (2)$$

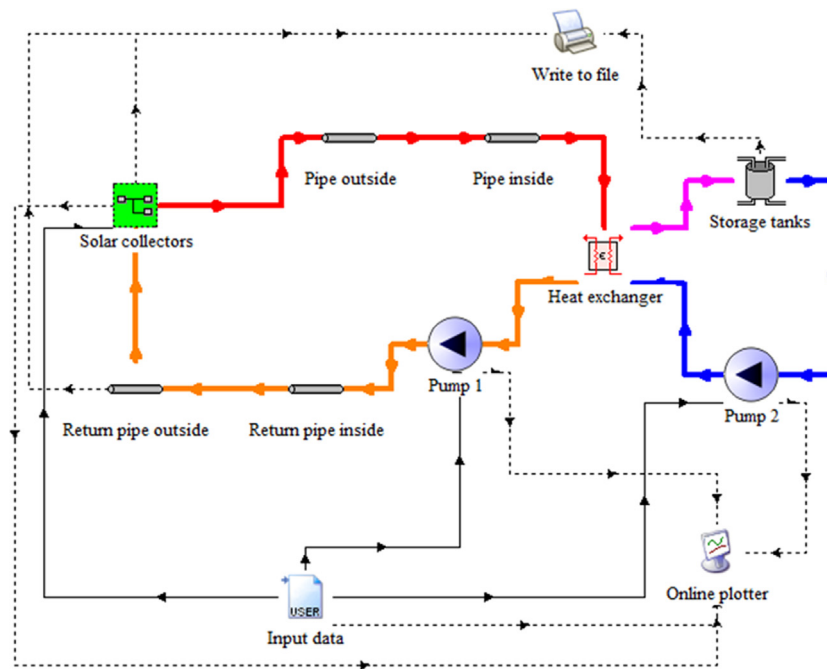
The term  $\dot{Q}_j$  represents the time rate of heat transfer at the location of the boundary of the control volume, where the instantaneous temperature is  $T_j$ .

The total specific exergy of the  $i$ -th material stream is calculated by [29]:

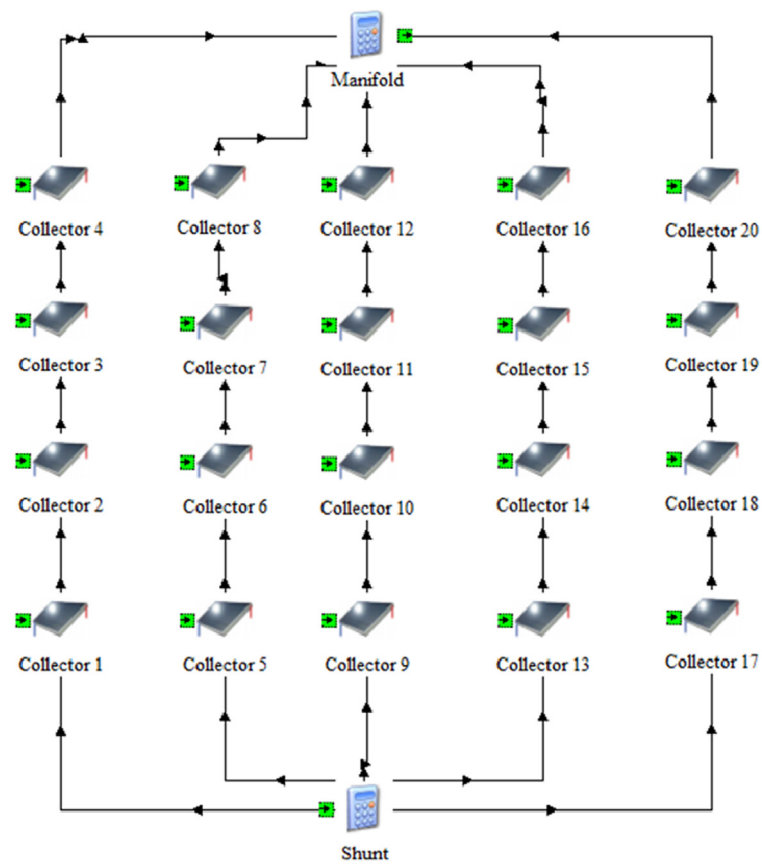
$$ex_i = ex_i^{PH} + ex_i^{CH} + ex_i^{KN} + ex_i^{PT} \quad (3)$$

Here, the potential,  $ex_i^{PT}$ , and kinetic,  $ex_i^{KN}$ , exergies have been neglected. Neither the chemical exergy,  $ex_i^{CH}$ , has been considered, because the composition of the circulating fluid is assumed to be constant during the process. Therefore, the exergy of the  $i$ -th material stream is obtained from the specific physical exergy,  $ex_i^{PH}$ , and its mass flow rate,  $\dot{m}_{fluid}$  [29]:

$$\dot{E}x_i = \dot{E}x_i^{PH} = \dot{m}_{fluid} [(h_i - h_0) - T_0 (s_i - s_0)] \quad (4)$$



a)



b)

Fig. 3 Scheme of the dynamic model: (a) General view of the model; (b) Detail of the connection among the solar collectors.

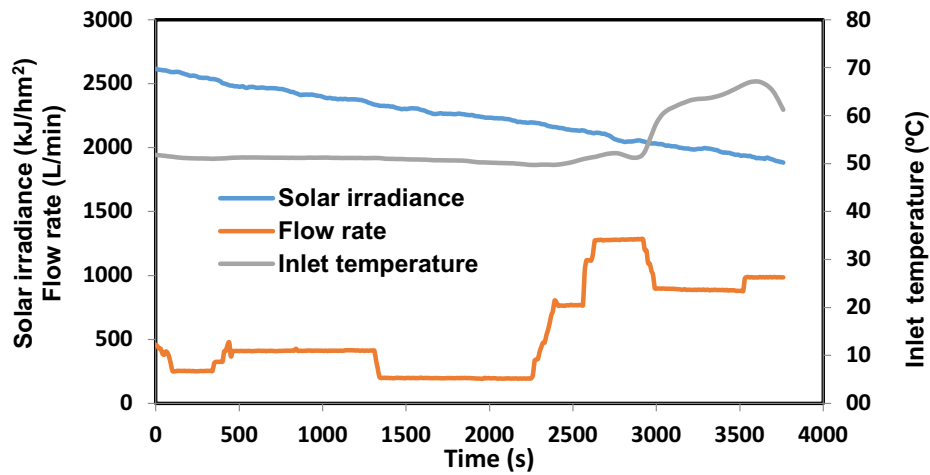


Fig. 4 Evolution of solar irradiance, flow rate and inlet temperature during tests.

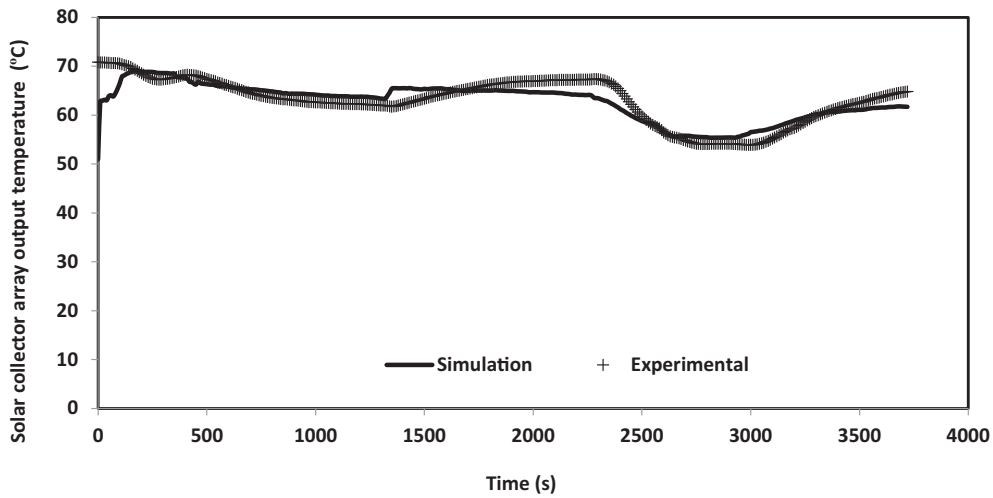


Fig. 5 Comparison between simulated and experimental solar collector array output temperature.

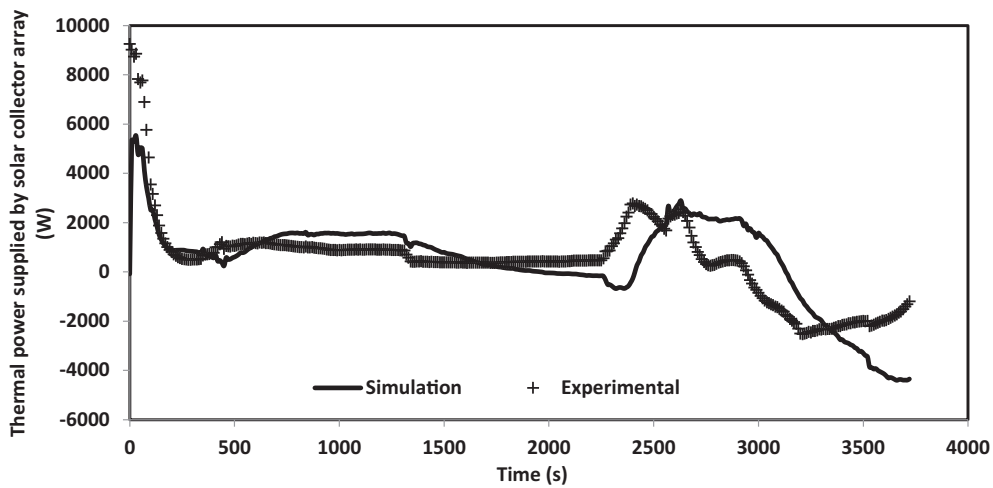


Fig. 6 Comparison between simulated and experimental thermal power supplied by the solar collector array.

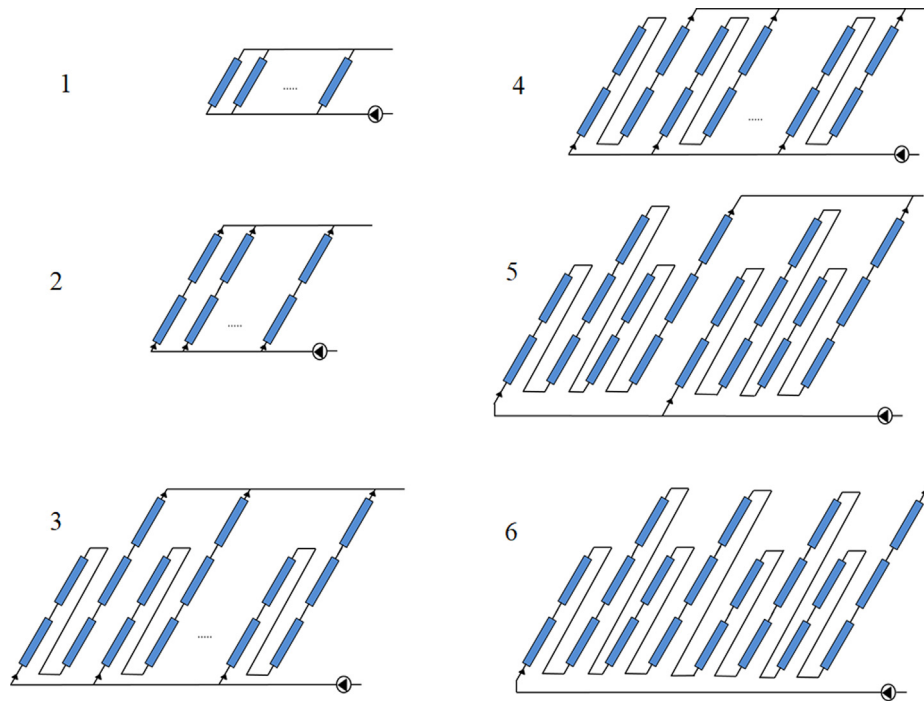


Fig. 7 Solar collector array configurations analysed.

**Table 1** Codes for array configuration and irradiance levels.

Configuration	
1	20 collectors in parallel
2	10 branches of 2 collectors in series
3	5 branches of 4 collectors in series
4	4 branches of 5 collectors in series
5	2 branches of 10 collectors in series
6	20 collectors in series
Irradiance	
A	200 (W/m <sup>2</sup> )
B	400 (W/m <sup>2</sup> )
C	600 (W/m <sup>2</sup> )
D	800 (W/m <sup>2</sup> )
E	1000 (W/m <sup>2</sup> )

The circulating fluid remains in a liquid phase during the process, so that [29]:

$$\dot{E}x_i = \dot{m}_{fluid} \left[ c_p(T_i - T_0) - T_0 c_p \ln\left(\frac{T_i}{T_0}\right) + T_0 R \ln\left(\frac{p_i}{p_0}\right) \right]. \quad (5)$$

For the exergy reference environment, the temperature and pressure in Gijón during the experimental test have been taken as  $T_0 = 19$  °C,  $p_0 = 1022.5$  mbar. The system boundaries are located outside the device, where the temperature corresponds to the ambient temperature, taken here as the temperature of the exergy reference environment,  $T_0$ . This way, there is no heat transfer to the environment, and the exergy loss term just refers to material wastes. Therefore, exergy destruction term

accounts for the total exergy destruction within the component: exergy destruction due to the friction and the irreversibility of heat transfer within the control volume.

For the calculation of the exergetic efficiency, the following definition has been taken [30]:

$$\eta_{ex} = \frac{\dot{E}x_P}{\dot{E}x_F} = 1 - \frac{\dot{E}x_D - \dot{E}x_L}{\dot{E}x_F}. \quad (6)$$

Applying the exergetic balance to the different components of the installation (Fig. 2):

Solar collectors:

$$\dot{E}x_{i,in} + \dot{E}x_{sr} = \dot{E}x_{i,out} + \dot{E}x_{D,collector}. \quad (7)$$

The exergy of the solar radiation [31] is:

$$\dot{E}x_{sr} = A_c \hat{A} \cdot I \left[ 1 - \frac{4}{3} \left( \frac{T_0}{T_s} \right) + \frac{1}{3} \left( \frac{T_0}{T_s} \right)^4 \right], \quad (8)$$

where  $A_c$  is the collector area (1.91 m<sup>2</sup>),  $I$  the solar irradiance (200, 400, 600, 800, and 1000 W/m<sup>2</sup>), and  $T_s$  the apparent black body temperature of the sun, which is assumed to be 5777 K.

In the solar collectors, the exergy of the fuel is the exergy of the solar radiation, and the exergy of the product the increase in exergy of the circulating fluid streams. Therefore:

$$\eta_{ex,collector} = \frac{\dot{E}x_{i,out} - \dot{E}x_{i,in}}{\dot{E}x_{sr}}. \quad (9)$$

Heat Exchanger:

$$\dot{E}x_3 + \dot{E}x_5 = \dot{E}x_4 + \dot{E}x_6 + \dot{E}x_{D,HX}. \quad (10)$$

In the heat exchanger, the primary circuit transfers exergy to the secondary circuit. This way:

$$\eta_{ex,HX} = \frac{\dot{E}x_3 - \dot{E}x_4}{\dot{E}x_6 - \dot{E}x_5} \quad (11)$$

Water tank:

In the tank some heat is transferred to the supply water. So, the exergy balance becomes:

$$\dot{E}x_6 + \dot{E}x_7 = \dot{E}x_5 + \dot{E}x_8 + \dot{E}x_{D,Deposit} \quad (12)$$

And,

$$\eta_{ex,Deposit} = \frac{\dot{E}x_8 - \dot{E}x_7}{\dot{E}x_6 - \dot{E}x_5} \quad (13)$$

Total system:

$$\dot{E}x_{sr} + \dot{E}x_7 = \dot{E}x_Q + \dot{E}x_8 + \dot{E}x_{D,tot} \quad (14)$$

As a result of the whole process, the exergy of the solar radiation is transferred to the supply water:

$$\eta_{ex,tot} = \frac{\dot{E}x_8 - \dot{E}x_7}{\dot{E}x_{sr}} \quad (15)$$

### 5. Results and discussion

Both the energetic and the exergetic efficiencies of the collector array for the different scenarios have been analysed and compared. *EES* (Engineering Equation Solver) Software has been used for the calculations. Fig. 8 and Fig. 9 show, under irradi-

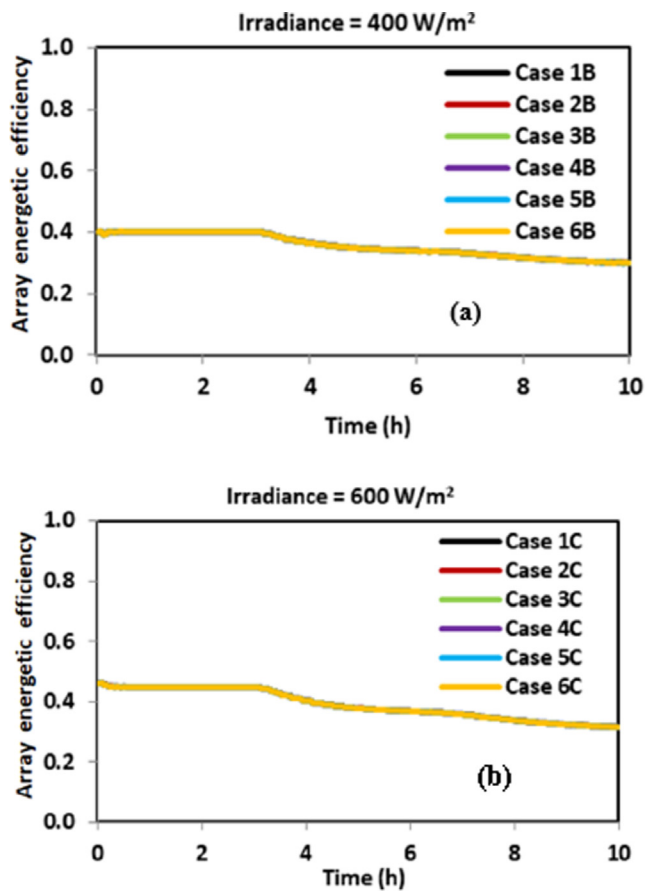


Fig. 8 Energetic efficiency of the array for the analysed configurations under irradiances of a) 400 W/m<sup>2</sup> and b) 600 W/m<sup>2</sup>.

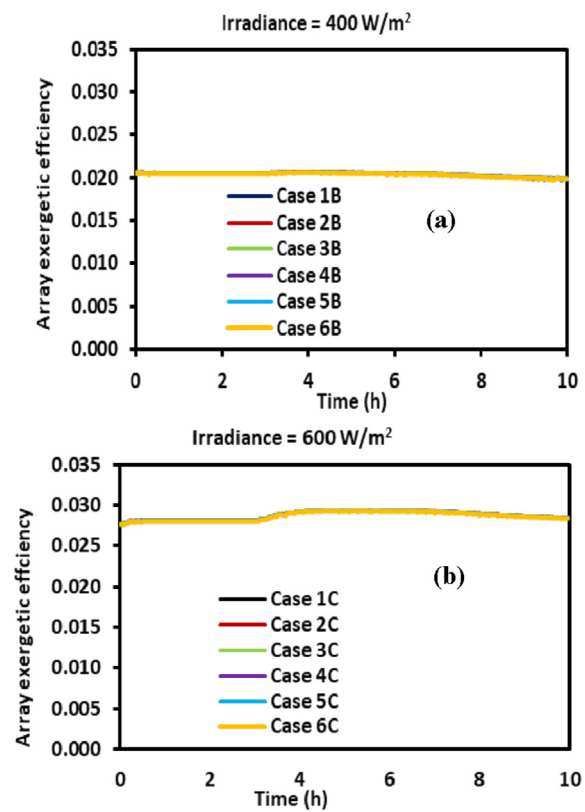
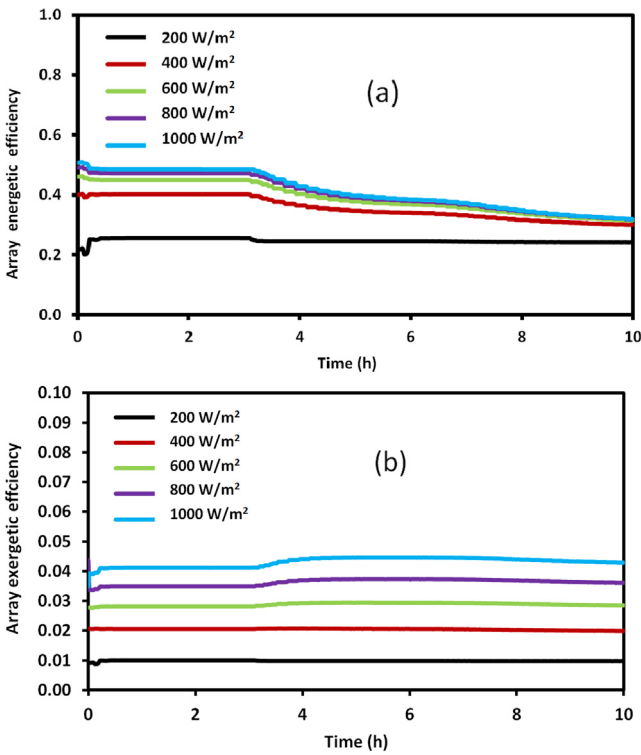


Fig. 9 Exergetic efficiency of the array for the analysed configurations under irradiances of a) 400 W/m<sup>2</sup> and b) 600 W/m<sup>2</sup>.

ances of 400 and 600 W/m<sup>2</sup>, the energetic and exergetic efficiency of the arrays as a function of time, respectively. And Fig. 10 shows the energetic and exergetic efficiency of the arrays also as a function of time versus the irradiance. These irradiance levels were selected because they are the most frequent in the location where the installation was tested.

The values of the exergetic efficiency of the collectors are always very low (within 1% and 4.6%), no matter the configuration nor the irradiance, as shown in Fig. 9 and Fig. 10b. Other authors have obtained similar results [8,32,33,34], which is justified by the high energy (and, therefore, exergy) leaks to the environment in the collector [32]. In particular, the high exergetic loss is caused by the following factors: a) heat release from the absorber plate to the surrounding environment, b) difference in temperature across the surface of the absorber plate and the sun, c) solar radiation leaks from the collector surface to the absorber plate, and d) temperature difference between absorber plate and fluid [21].

For all the irradiance levels studied, the configuration does not affect neither the energetic nor the exergetic efficiency of the collectors' array, as it can be seen in Fig. 7 and Fig. 8 for irradiance levels of 400 and 600 W/m<sup>2</sup>. The reason for these results is that the mass flow rate of the primary circuit was kept constant whatever the configuration. This condition results in high mass flow rates inside the collectors in the series configurations, which leads to high pressure losses that make these configurations unfeasible in practical installations but they were still considered for conceptual reasons. It is commonly known that series connections are used with small flow rates obtaining high temperatures and thus the collector efficiency



**Fig. 10** a) Array energetic efficiency and b) array exergetic efficiency versus irradiance.

is penalized. However, if high flow rates could be assumed in the installation, it could be possible to obtain the same efficiency with a series configuration as with parallel.

With regard to the irradiance, it has been observed for all the configurations that the higher the irradiance, the higher both the energetic and the exergetic efficiencies, as it can be seen in Fig. 10. It can also be observed that as time goes by, and the fluid temperature increases, on one hand, the energetic efficiency decreases to a value independent of the irradiance, with the exception of the simulations with 200 W/m<sup>2</sup>, in which case the irradiance level is not high enough to increase the primary fluid temperature, and for this reason efficiency remains constant all over the simulation time. On the other hand, the exergetic efficiency first increases as the fluid temperature increases, but it starts to decrease once a maximum value is reached. This maximum is met after about 5 h of operation and it is not found in the simulations with 200 W/m<sup>2</sup>, where, as already mentioned, the temperature of the primary fluid remains practically unchanged. The same trend is observed by other authors [21,32]. The reason for this is that after 5 h of operation an optimum fluid inlet temperature is met, at which the exergetic efficiency of the array reaches a maximum value (Fig. 11). The increase of the collector inlet temperature rises both the outlet temperature and the average absorber plate temperature, and, in this way, opposite effects are obtained. The exergetic efficiency is more affected by the outlet temperature at low temperatures and becomes higher with it. But, at the same time, the rising of the average absorber plate temperature, increases the heat loss, which negatively impacts the exergetic efficiency and it is reduced [21].

As the simulation considers each collector as an independent element, it is possible to estimate input and output

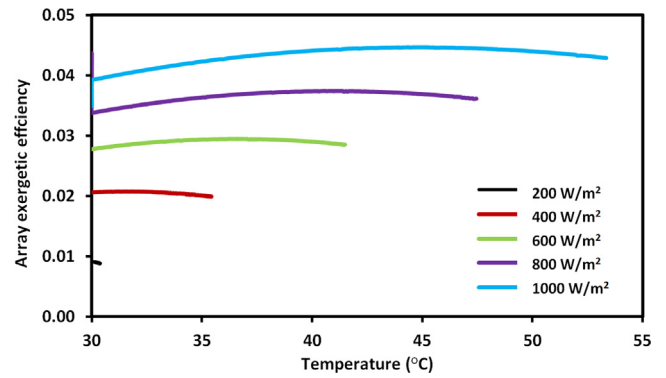


**Fig. 11** Array exergetic efficiency vs fluid inlet temperature and irradiance.

temperatures of each individual collector, and, thus estimating its efficiency individually. It must be noticed that as all collectors are assumed to be the same, and the mass flow is equally distributed in parallel branches, all collectors connected in parallel have the same performance. As an example, the individual efficiencies obtained in case 4C (4 branches of five collectors connected in series) are presented here. In Fig. 12, where the collector efficiency is presented as a function of time, collector 1 refers to the first collector of each branch, and collector 5 is the last one. As it can be seen, the energetic efficiency decreases as the fluid is passing through the collectors in series. This is due to the higher temperature of the fluid in each collector. Fig. 13 shows the fluid mean temperature of the different collectors connected in series for this simulation case, and a temperature difference of 5–10 °C is observed between the first and the last collectors in the branch.

The evolution of the exergetic efficiency presents a different trend. Fig. 14 shows the exergetic efficiency as a function of time and fluid inlet temperature for the 4C simulation. Initially, the higher the fluid inlet temperature, the higher the exergetic efficiency of the collector. But, once again, we are in the presence of the opposite effect that the increase in fluid inlet temperature over time has on exergetic performance. At low fluid inlet temperatures, the exergetic efficiency meets a maximum value as the inlet temperature increases. This behaviour can be observed in collectors from 2 to 4, and in the average of the 5 collectors in series. In collector 1, the initial inlet

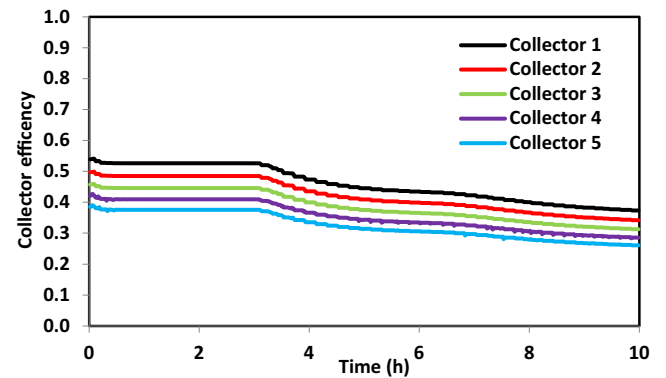


**Fig. 12** Individual energetic collector efficiency for case 4C simulation.

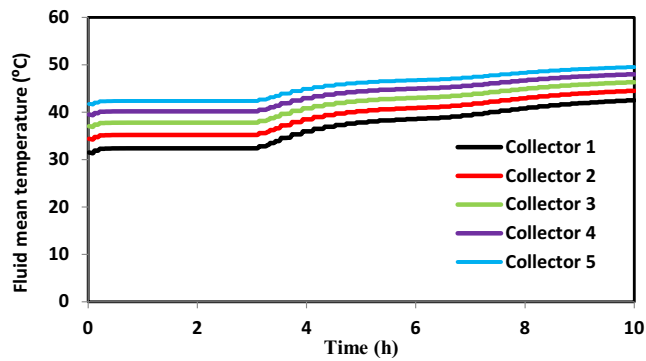


Fig. 13 Fluid mean temperature for each collector for case 4C simulation.

temperature is very low, and the exergetic efficiency grows constantly, because the exergy increase of the fluid is higher than the exergy loss due to heat leaks. But, in collector 5, the fluid inlet temperature is too high, and the negative effect of the heat

loss negatively affects the exergetic efficiency from the beginning of the simulation.

As the solar arrays belong to a general installation, where heat is transferred to the water supply of a residential building, it is appropriate to consider the evolution of the performance of the other main devices as well. Fig. 15 shows the exergetic efficiency of the plate heat exchanger (HX) and the water storage tank as a function of time for the different irradiances. In this study, the efficiencies of these two components do not vary with the configuration of the solar system since the main global parameters of the installation do not change either. The plate heat exchanger presents high exergetic efficiencies values because no heat losses to the environment have been considered. Initially, the higher the irradiance, the lower the exergetic efficiency of the HX, but it grows over time, and, until after 8 h of operation, all cases have similar values. The exergetic efficiency of the water tank grows steadily over time for all irradiances, as expected. The only exception to the general behaviour is case 200 W/m<sup>2</sup>, but it is not representative, because the temperature of the input fluid barely changes.

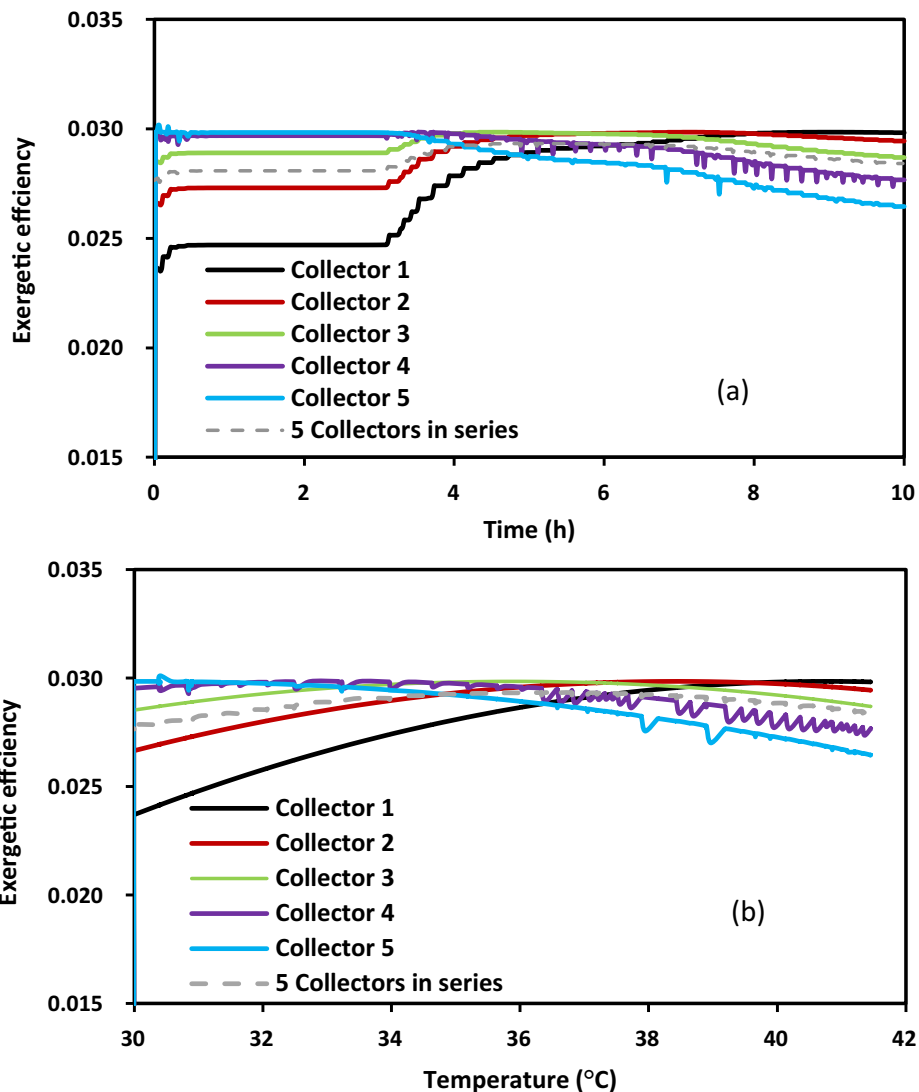
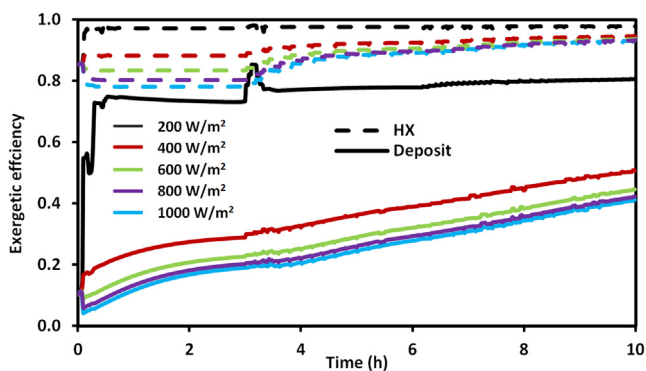
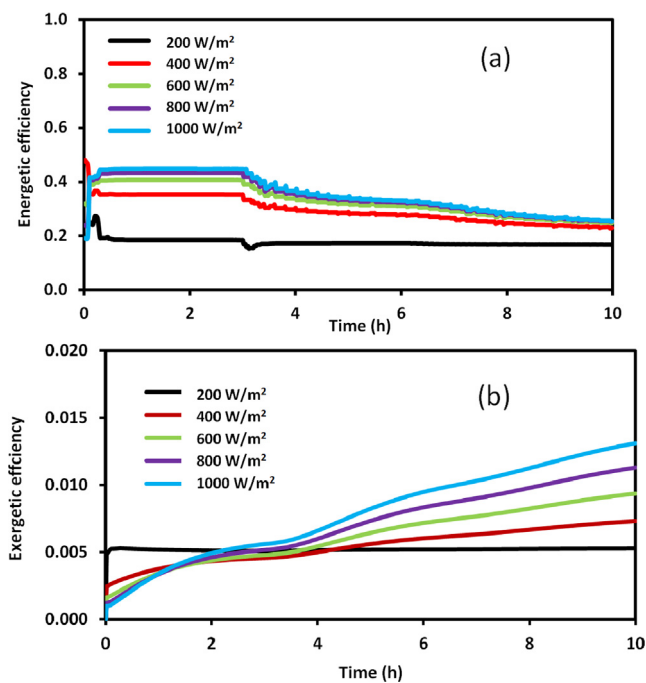


Fig. 14 Exergetic efficiency vs a) time and b) fluid inlet temperature for case 4C.



**Fig. 15** Heat exchanger and deposit exergetic efficiencies as a function of time at different irradiances.



**Fig. 16** Installation global efficiency a) energetic and b) exergetic.

If the complete installation is considered, the global efficiency can be analysed. As the only part of the installation that changes among simulation cases is the collector array configuration, and it has been shown that it has negligible influence on the array efficiency, the global efficiency of the installation is also independent of the configuration. The influence of the irradiance level on both the global energetic and exergetic efficiencies is shown in Fig. 16. The global energetic efficiencies have similar tendencies to the efficiencies of the arrays shown in Fig. 9, but with slightly lower values. Meanwhile, the exergetic efficiencies, with very low values ( $< 1.5\%$ ), now no longer show a maximum, but grow steadily over time, except for case  $200 \text{ W/m}^2$ , where it remains the same, as explained above.

## 6. Conclusions

A solar thermal installation of 20 flat-plate collectors at the Gijón Solar Cooling Laboratory (GSCL) has been modelled

and validated with experimental data, and six different configurations (series and parallel) of the collector array have been analysed, under five different normal irradiance conditions ( $200, 400, 600, 800$  and  $1000 \text{ W/m}^2$ ), giving a total of 30 cases.

The values of the exergetic efficiency of the collectors are always very low (within  $1\%$  and  $4.6\%$ ), no matter neither the configuration nor the irradiance, justified by the high exergy leaks to the environment. No significant differences on both energetic and exergetic efficiency were found for the series and parallel configurations, as the primary circuit mass flow rate was kept constant for all the simulations. If pressure losses were acceptable for the series configuration, the same efficiency as for parallel configuration could be achieved.

The evolution of exergetic efficiency with time shows that a maximum efficiency exists, after 5 h of operation. As time goes by, the collector temperature rises causing the exergetic output to increase but, also, the thermal losses. Therefore, an optimum collector temperature is reached where exergetic efficiency is maximized. This is a difference with respect to the energetic efficiency, which always decreases whereas the collector temperature increases. With regard to the irradiance, it has been observed for all the configurations that the higher the irradiance, the higher both the energetic and exergetic efficiencies.

Global installation exergetic efficiency is governed by the tendency of the deposit efficiency, but with lower values due to the low collector exergetic efficiency, which agrees with the literature. The values of global energetic efficiency are in the range  $20\text{--}50\%$  for all the simulations, whereas the global exergetic efficiency is always lower than  $1.5\%$ .

Although the model results are satisfactory, it would be interesting in future works to improve its dynamical behavior, in order to achieve a more precise response compared to experiments. This improvement could make it possible to analyse high frequency phenomena such as the effect of transient cloud shading on the collectors.

## Declaration of Competing Interest

The authors declare that they have no known competing financial interests or personal relationships that could have appeared to influence the work reported in this paper.

## Acknowledgments

This research has been funded by ERDF funds, INTERREG MAC 2014-2020 programme, within the ACLIEMAC project (MAC2/3.5b/380). No funding sources had any influence on study design, collection, analysis, or interpretation of data, manuscript preparation, or the decision to submit for publication. The authors would like to thank all the companies and Institutions included in the ARFRISOL Singular Strategic Project.

## References

- [1] L.M. Ayompe, A. Duffy, S.J. McCormack, M. Conlon, Validated TRNSYS model for forced circulation solar water heating systems with flat-plate and heat pipe evacuated tube collectors, *Appl. Therm. Eng.* 31 (2011) 1536–1542, <https://doi.org/10.1016/j.applthermaleng.2011.01.046>.

- [2] A. Hobbi, K. Siddiqui, Optimal design of a forced circulation solar water heating system for a residential unit in cold climate using TRNSYS, *Sol. Energy*. 83 (2009) 700–714, <https://doi.org/10.1016/j.solener.2008.10.018>.
- [3] F. Bava, S. Furbo, Development and validation of a detailed TRNSYS-Matlab model for large solar collector fields for district heating applications, *Energy* 135 (2017) 698–708, <https://doi.org/10.1016/j.energy.2017.06.146>.
- [4] Z. Tian, B. Perers, S. Furbo, J. Fan, Thermo-economic optimization of a hybrid solar district heating plant with flat plate collectors and parabolic trough collectors in series, *Energy Convers. Manag.* 165 (2018) 92–101, <https://doi.org/10.1016/j.enconman.2018.03.034>.
- [5] K.M. Pandey, R. Chaurasiya, A review on analysis and development of solar flat plate collector, *Renew. Sustain. Energy Rev.* 67 (2017) 641–650, <https://doi.org/10.1016/j.rser.2016.09.078>.
- [6] S.K. Verma, A.K. Tiwari, D.S. Chauhan, Experimental evaluation of flat plate solar collector using nanofluids, *Energy Convers. Manag.* 134 (2017) 103–115, <https://doi.org/10.1016/j.enconman.2016.12.037>.
- [7] W. Xiaowu, H. Ben, Exergy analysis of domestic-scale solar water heaters, *Renew. Sustain. Energy Rev.* 9 (2005) 638–645, <https://doi.org/10.1016/j.rser.2004.04.007>.
- [8] E. Zambolin, D. Del Col, Experimental analysis of thermal performance of flat plate and evacuated tube solar collectors in stationary standard and daily conditions, *Sol. Energy*. 84 (2010) 1382–1396, <https://doi.org/10.1016/j.solener.2010.04.020>.
- [9] A. Alvarez, O. Cabeza, M.C. Muñiz, L.M. Varela, Experimental and numerical investigation of a flat-plate solar collector, *Energy*. 35 (2010) 3707–3716, <https://doi.org/10.1016/j.energy.2010.05.016>.
- [10] R.L. Shrivastava, V. Kumar, S.P. Untawale, Modeling and simulation of solar water heater: A TRNSYS perspective, *Renew. Sustain. Energy Rev.* 67 (2017) 126–143, <https://doi.org/10.1016/j.rser.2016.09.005>.
- [11] L.A. Tagliafico, F. Scarpa, M. De Rosa, Dynamic thermal models and CFD analysis for flat-plate thermal solar collectors - A review, *Renew. Sustain. Energy Rev.* 30 (2014) 526–537, <https://doi.org/10.1016/j.rser.2013.10.023>.
- [12] T. Sokhansefat, A. Kasaean, K. Rahmani, A.H. Heidari, F. Aghakhani, O. Mahian, Thermo-economic and environmental analysis of solar flat plate and evacuated tube collectors in cold climatic conditions, *Renew. Energy*. 115 (2018) 501–508, <https://doi.org/10.1016/j.renene.2017.08.057>.
- [13] A.K. Tiwari, S. Gupta, A.K. Joshi, F. Raval, M. Sojitra, TRNSYS simulation of flat plate solar collector based water heating system in Indian climatic condition, *Mater. Today: Proc.* (2020), <https://doi.org/10.1016/j.matpr.2020.08.794>. (In Press).
- [14] I. Harrabi, M. Hamdi, A. Bessifi, M. Hazami, Dynamic modelling of solar thermal collectors for domestic hot water production using TRNSYS, *Euro-Mediterranean J. Environ. Integr.* (2021) 6–21, <https://doi.org/10.1007/s41207-020-00223-6>.
- [15] Z. Tian, B. Perers, S. Furbo, J. Fan, Analysis and validation of a quasi-dynamic model for a solar collector field with flat plate collectors and parabolic trough collectors in series for district heating, *Energy* 142 (2018) 130–138, <https://doi.org/10.1016/j.energy.2017.09.135>.
- [16] H. Gunerhan, A. Hepbasli, Exergetic modeling and performance evaluation of solar water heating systems for building applications, *Energy Build.* 39 (2007) 509–516, <https://doi.org/10.1016/j.enbuild.2006.09.003>.
- [17] S. Farahat, F. Sarhaddi, H. Ajam, Exergetic optimization of flat plate solar collectors, *Renew. Energy*. 34 (2008) 1169–1174, <https://doi.org/10.1016/j.renene.2008.06.014>.
- [18] M. Pons, Exergy analysis of solar collectors, from incident radiation to dissipation, *Renew. Energy*. 47 (2012) 194–202, <https://doi.org/10.1016/j.renene.2012.03.040>.
- [19] F. Jafarkazemi, E. Ahmadifard, Energetic and exergetic evaluation of flat plate solar collectors, *Renew. Energy*. 56 (2013) 55–63, <https://doi.org/10.1016/j.renene.2012.10.031>.
- [20] Sunil Chamoli, Exergy analysis of a flat plate solar collector, *J. Energy South. Africa*. 24 (2013) 8–13.
- [21] Z. Ge, H. Wang, H. Wang, S. Zhang, X. Guan, Exergy Analysis of Flat Plate Solar Collectors, *Entropy*. 16 (2014) 2549–2567, <https://doi.org/10.3390/e16052549>.
- [22] A. Mortazavi, M. Ameri, Conventional and advanced exergy analysis of solar flat plate air collectors, *Energy*. 142 (2018) 277–288, <https://doi.org/10.1016/j.energy.2017.10.035>.
- [23] A.M. Genc, M.A. Ezan, A. Turgut, Thermal performance of a nanofluid-based flat plate solar collector: A transient numerical study, *Appl. Therm. Eng.* 130 (2018) 395–407, <https://doi.org/10.1016/j.applthermaleng.2017.10.166>.
- [24] S.A. Kalogirou, S. Karellas, K. Braimakis, C. Stanciu, V. Badescu, Exergy analysis of solar thermal collectors and processes, *Prog. Energy Combust. Sci.* 56 (2016) 106–137, <https://doi.org/10.1016/j.pecs.2016.05.002>.
- [25] S. Rosiek, Exergy analysis of a solar-assisted air-conditioning system: Case study in southern Spain, *Appl. Therm. Eng.* 148 (2019) 806–816, <https://doi.org/10.1016/j.applthermaleng.2018.10.132>.
- [26] S.A. Sakhaei, M.S. Valipour, Performance enhancement analysis of the flat plate collectors: A comprehensive review, *Renew. Sustain. Energy Rev.* 102 (2019) 186–204, <https://doi.org/10.1016/j.rser.2018.11.014>.
- [27] A. Allouhi, M.B. Amine, M.S. Buker, T. Kousksou, A. Jamil, Forced-circulation solar water heating system using heat pipe-flat plate collectors: Energy and exergy analysis, *Energy*. 180 (2019) 429–443, <https://doi.org/10.1016/j.energy.2019.05.063>.
- [28] TRNSYS, TRNSYS 17a TRaNsient System Simulation program, Vol. 4 Math. Ref. (2020). [25] A. Bejan, *Advanced engineering thermodynamics*, 2nd ed., Wiley, New York, 1988.
- [29] A. Bejan, *Advanced engineering thermodynamics*, second ed., Wiley, New York, 1988.
- [30] A. Bejan, G. Tsatsaronis, M. Moran, *Thermal design and optimization*, Wiley, New York, 1996.
- [31] R. Petela, *Engineering Thermodynamics of Thermal Radiation (For Solar Power Utilization)*, first ed., Mc Graw-Hill, New York, 2010.
- [32] I.P. Koronaki, M.T. Nitsas, Experimental and theoretical performance investigation of asymmetric photovoltaic/thermal hybrid solar collectors connected in series, *Renew. Energy*. 118 (2018) 654–672, <https://doi.org/10.1016/j.renene.2017.11.049>.
- [33] R. Daghighi, A. Shafieian, Theoretical and experimental analysis of thermal performance of a solar water heating system with evacuated tube heat pipe collector, *Appl. Therm. Eng.* 103 (2016) 1219–1227, <https://doi.org/10.1016/j.applthermaleng.2016.05.034>.
- [34] K. Balaji, S. Iniyar, M.V. Swami, Exergy, economic and environmental analysis of forced circulation flat plate solar collector using heat transfer enhancer in riser tube, *J. Clean. Prod.* 171 (2018) 1118–1127, <https://doi.org/10.1016/j.jclepro.2017.10.093>.